49. K. McCormack, T. McCormack, M. Tanouye, B. Rudy, W. Stuhmer, *FEBS Lett.* **370**, 32 (1995).
50. G. Shi *et al.*, *Neuron* **16**, 843 (1996).
51. N. Nagaya, D. M. Papazian, *J. Biol. Chem.* **272**, 3022 (1997).
52. T. A. Jones, J. Y. Zou, S. W. Cowan, M. Kjeldgaard, *Acta Crystallogr.* **A47**, 110 (1991).
53. M. Carson, *Methods Enzymol.* **277**, 493 (1997).
54. P. Kraulis, *J. Appl. Crystallogr.* **24**, 946 (1991).
55. A. Nicholls, K. A. Sharp, B. Honig, *Proteins* **11**, 281 (1991).
56. We thank A. Lee, V. Ruta, and members of the MacKinnon laboratory for helpful discussions; R. Jain for initial experiments with lipids; Q. Wang and B. T. Chait for mass spectrometry; R. Dutzler for assistance with data collection; O. Pongs for Kv1.2 DNA; J. Trimmer for β_2 subunit DNA; Brookhaven National Laboratory (National Synchrotron Light Source beamlines X25 and X29) and the Swiss Light Source (beamline PX1) staff for assistance in data collection; and W. Chin for help with manuscript preparation. This work was supported in part by NIH grant no. GM43949 to R.M. and NIH grant no. RR00862 to B. T. Chait. R.M. is an Investigator in the Howard Hughes Medical Institute. Atomic coordinates and structure factors have been deposited with the Protein Data Bank with accession ID 2A79.

Supporting Online Material
www.sciencemag.org/cgi/content/full/1116269/DC1
Materials and Methods
References

17 June 2005; accepted 5 July 2005
Published online 7 July 2005;
10.1126/science.1116269
Include this information when citing this paper.

Voltage Sensor of Kv1.2: Structural Basis of Electromechanical Coupling

Stephen B. Long, Ernest B. Campbell, Roderick MacKinnon*

Voltage-dependent ion channels contain voltage sensors that allow them to switch between nonconductive and conductive states over the narrow range of a few hundredths of a volt. We investigated the mechanism by which these channels sense cell membrane voltage by determining the x-ray crystal structure of a mammalian *Shaker* family potassium ion (K^+) channel. The voltage-dependent K^+ channel Kv1.2 grew three-dimensional crystals, with an internal arrangement that left the voltage sensors in an apparently native conformation, allowing us to reach three important conclusions. First, the voltage sensors are essentially independent domains inside the membrane. Second, they perform mechanical work on the pore through the S4-S5 linker helices, which are positioned to constrict or dilate the S6 inner helices of the pore. Third, in the open conformation, two of the four conserved Arg residues on S4 are on a lipid-facing surface and two are buried in the voltage sensor. The structure offers a simple picture of how membrane voltage influences the open probability of the channel.

Voltage-dependent ion channels open in response to changes in voltage across the cell membrane (*1*). In this process, the membrane electric field performs mechanical work to alter the channel's conformation within the membrane. The work arises from the force exerted by the electric field on charged amino acids, termed gating charges (*1–3*). The size of the gating charge is very large (*4*), accounting for the exquisite sensitivity of voltage-dependent ion channels to small changes in membrane voltage. To understand this process, one must first answer two questions: How do gating charges move within the membrane electric field? And how are these movements mechanically coupled to opening and closing of the pore?

No experimentally based model has yet provided answers to both of these questions. So far, little progress has been made toward the second question concerning the mechanical coupling of voltage-sensor movements to the pore. Most effort has focused on how the gating charges move; the main subject of study has been the *Shaker* voltage-dependent K^+ (Kv) channel, and numerous models have been put forth. One fundamental constraint for any model is that when a *Shaker* K^+ channel opens, it transfers the net equivalent of 12 to 14 positive elementary charges across the membrane electric field from inside to outside, and most of this charge is carried by four S4 Arg residues on each of four identical channel subunits (*4–6*).

A guiding assumption underlying most models for the voltage sensor has been that the S4 helix with its Arg residues is completely (*7–10*), or mostly (*11*), sequestered from the membrane, in order to protect the charges from the lipid's low dielectric environment. To accomplish this, most models postulate that the S4 helix inserts into a groove at the interface between adjacent subunits of the K^+ channel tetramer, such that pore α helices S5 and S6 form a wall on one side of S4 and voltage-sensor α helices S1 to S3 form a wall on the other side, the lipid-facing perimeter, to create a gating channel or protein-lined canaliculus for S4 (*7–10*, *12*). This arrangement would allow the S4 helix to move its charged amino acids across the membrane without exposing them to the lipid environment.

How and to what extent S4 moves has been the subject of much debate. Gating-dependent reactivity of sulfhydryl reagents with cysteine residues led to an initial hypothesis of large (~15 Å) translations of S4 in some models (*13–17*). But very small distance changes measured in fluorescence resonance energy transfer (FRET) experiments suggested much smaller movements of S4 across the membrane (*18*, *19*). Crevices surrounding S4 were invoked to account for the sulfhydryl reactivity in the setting of these smaller movements, with translations and/or rotations of S4 occurring across a narrow neck inside an hourglass-shaped canaliculus. In the transporter model hypothesis, the S4 does not change its depth in the membrane at all (less than 3 Å movement) (*18*, *20*). Instead, the field is moved over the S4 charges by alternately opening and closing crevices to the internal and external solutions.

The above models of voltage-dependent gating vary in detail, but they have had two essential features in common. First, the S4 helix is sequestered from the lipid membrane [although Larsson and colleagues proposed that a surface of S4 could be exposed to lipid (*11*)]. Second, the voltage-sensor helices S1 to S4 are packed tightly against the α helices of the pore. In other words, it was reasonably assumed that voltage-dependent ion channels are like conventional α-helical membrane proteins that form a fairly rigid disk of helices in the membrane. A first hint that a rigid disk of helices might not pertain to voltage-dependent ion channels came from the demonstration that the voltage sensor (S1 to S4) from the *Shaker* Kv channel could be spliced onto the pore of KcsA (a non–voltage-dependent K^+ channel) to confer voltage-dependent gating (*21*). This finding implied that the voltage sensor might be an almost-independent domain, because if it had to form a large interface through helix packing with the pore, the chimera would likely not function.

The first atomic structures of a prokaryotic Kv channel (KvAP) also implied that the voltage sensors are loosely attached to the pore (*22*). One of these [Protein Data Bank (PDB) ID 1ORS] was of an isolated voltage-sensor domain, which surprisingly could be expressed in the membrane by itself (without the pore). Another, which is a full-length channel structure (PDB ID 1ORQ), showed the voltage-

Howard Hughes Medical Institute, Laboratory of Molecular Neurobiology and Biophysics, Rockefeller University, 1230 York Avenue, New York, NY 10021, USA.

*To whom correspondence should be addressed. E-mail: mackinn@rockefeller.edu

sensor domains in a non-native conformation, pulled toward the cytoplasmic side of the pore. Not only had the voltage sensors undergone domain-like movements with respect to the pore, but the sensors seemed to have a great deal of internal flexibility. This was unusual behavior for a membrane protein. The Arg-containing S4 helix formed part of a helix-turn-helix structure (termed a voltage-sensor paddle) through its antiparallel relationship to S3b (the C-terminal half of S3). The paddle was proposed to move at the protein-lipid interface with S3b "above" and S4 "below." Experiments with avidin capture of biotin suggested that some of the Arg residues move more than 15 Å through the thickness of the membrane (*23*, *24*).

The KvAP studies implied that the voltage sensors are highly mobile; that S4 is not in a canaliculus; and possibly that some S4 Arg residues could be exposed to the lipid membrane, which would allow the voltage-sensing apparatus to exploit opposing electrostatic and hydrophobic forces to gate the channel (*23*, *25*). However, a major weakness of the KvAP studies was directly related to the voltage sensors' mobility: Distortions associated with extraction from the membrane left many aspects of the structure uncertain. Most notably, the connections between the voltage sensors and pore were disrupted. The crystals of Kv1.2 have maintained these connections and thus convey more definitive information on the mechanism of voltage-dependent gating.

Voltage-sensor structure: Relationship between Kv1.2 and KvAP. Electron density maps are weak in the region of the voltage sensor, relative to the remainder of the channel. However, the four transmembrane helices (S1 to S4) were easily recognizable, with side-chain density for some, but not all, amino acids (*26*). Electron density was present for the first (Arg^{294}), second (Arg^{297}), and third (Arg^{300}) Arg residues on S4, and for two Phe residues (Phe^{302} and Phe^{305}), establishing the correct register of this helix (Fig. 1). The partial model of the voltage sensor contains helices for S1 (19 amino acids), S2 (residues 219 to 243), S3 (21 amino acids), S4 (residues 288 to 311), and the S4-S5 linker (residues 312 to 325). Com-

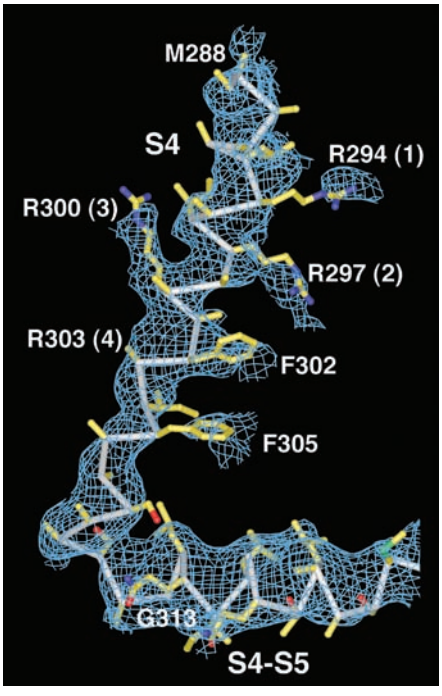

Fig. 1. Density for S4 and the S4-S5 linker calculated without a voltage-sensor model. The electron density map for S4 and the S4-S5 linker (blue mesh) is shown with the final model drawn as a C_α trace (gray) with side-chain residues (yellow, blue, and red sticks). Arg (R) residues 1 to 3 on S4 have density for their side chains. Density for these side chains and for two Phe residues (F302 and F305) helped establish the correct register of the S4 helix. The side chain of Arg 4 is truncated after the C_β atom (modeled as alanine) because density past this point was not present in the maps. A few other residues in S4 have also been modeled as alanine. Phases for the map were calculated by removing the entire voltage sensor (S1 to S4 helices through residue 313 of the S4-S5 linker) from the model and refining the remaining partial structure of the pore and T1/β complex using a simulated annealing protocol in the CNS software (*41*). This procedure, which is used to generate a "simulated annealing omit map," essentially eliminates bias in the map. The map is a $2F_o$-F_c map (where F_o is the observed structure factor and F_c is the calculated structure factor) that was calculated from 30 to 2.9 Å, contoured at 0.5σ, and drawn around the portion of the molecule shown. M, Met; G, Gly.

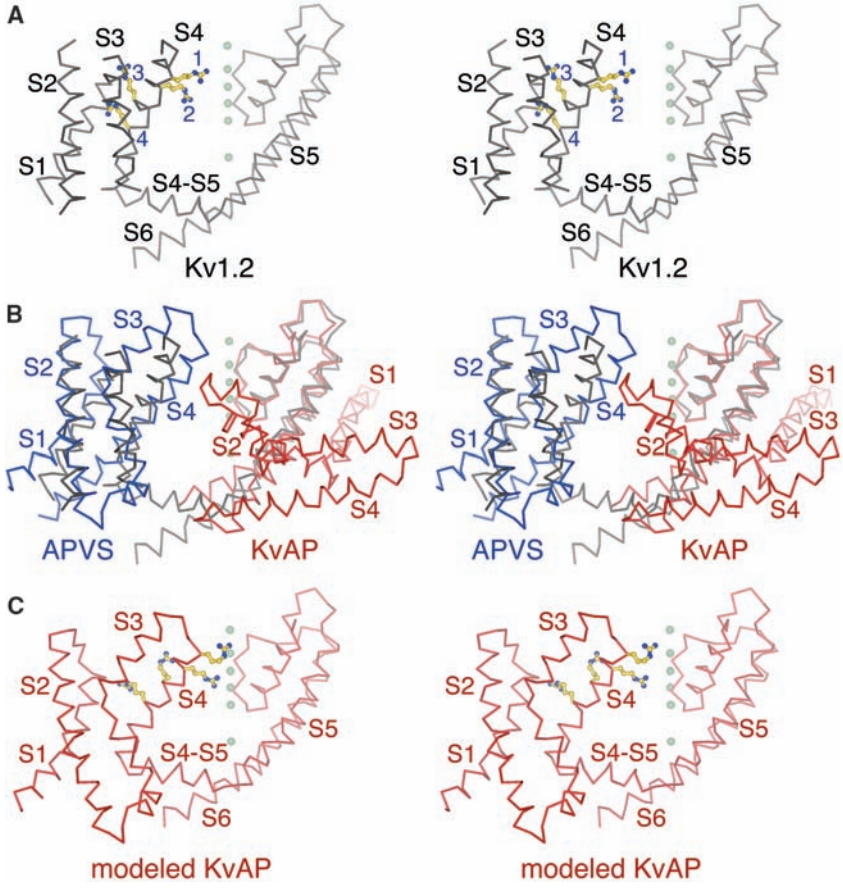

Fig. 2. Stereoviews comparing the Kv1.2 structure with two structures of the prokaryotic Kv channel KvAP. (**A**) A single subunit of the integral membrane pore and partial model of the voltage sensor of Kv1.2 viewed from the side as a gray C_α trace. Arg residues 1 to 4 on the S4 helix (blue labels) are depicted as yellow and blue sticks. The side chain for Arg 4, although not included in the final coordinates, is modeled in a chemically reasonable conformation for the purpose of illustration. (**B**) The Kv1.2 structure (gray) viewed as in (A) with a full-length crystal structure of KvAP (red C_α trace, PDB ID 2A0L) superimposed by alignment of main-chain atoms of the pore helices and selectivity filter, and with an isolated voltage-sensor structure of KvAP (Aeropyrum Pernix Voltage Sensor, or APVS) (blue C_α trace, PDB ID 1ORS) (*22*) superimposed by alignment of main-chain atoms of α helices S1 and S2. (**C**) A hypothetical model of a single KvAP subunit is shown as a red C_α trace with yellow and blue side chains for Arg residues 1 to 4 on the S4 helix. This was constructed by combining the isolated voltage sensor and pore of KvAP according to their positions relative to Kv1.2 as displayed in (B). The S4-S5 linker residues of KvAP (residues 136 to 146) are positioned relative to the pore and voltage sensor based on the Kv1.2 S4-S5 helix. A queue of K^+ ions (green spheres) from the pore are shown as a reference in (A) to (C). The figure was generated with Molscript software (*42*).

parisons with KvAP crystal structures assisted in the identification of these helices. Most side chains were included on S4, the S4-S5 linker, and S2. S1 and S3 were built with alanine residues. Loops connecting helices S1 to S2 and S3 to S4 were omitted because electron density was weak or absent. The turn connecting S2 to S3, which varies in its conformation in different crystal structures of KvAP (*22*) (and see PDB ID 2A0L), was also omitted. Thus, this partial model of the voltage sensor is missing several elements, but it still addresses many important questions.

A model of a single subunit of Kv1.2 is shown in Fig. 2A. Two different crystal structures of KvAP superimposed on Kv1.2 show the relationship between these channels (Fig. 2B). A full-length KvAP structure (PDB ID 2A0L, red) is aligned with the pore of Kv1.2, and an isolated voltage-sensor structure of KvAP [PDB ID 1ORS, blue (*22*)] is aligned with the voltage sensor of Kv1.2. A model of KvAP can be made to look like Kv1.2 by simply repositioning its voltage sensor to more closely resemble the isolated voltage-sensor structure (Fig. 2C). The linker connecting the voltage sensor to the pore in KvAP is the appropriate length and has the correct amphipathicity (see below) to match the linker in Kv1.2. Apparently, upon extraction of KvAP from the lipid membrane, the voltage sensor is dislodged from its proper position. This kind of distortion in multiple crystal structures of KvAP (*22*) (and see PDB ID 2A0L) probably reflects the importance of a cell membrane to hold the voltage sensor in its proper position. In Kv1.2, the presence of a T1 domain and its connection to the S1 helix undoubtedly help to maintain a native conformation of the voltage sensor.

We conclude that the basic architecture of the voltage sensor in a membrane is similar in Kv1.2 and KvAP. They both have an antiparallel arrangement of S3 and S4. This arrangement was called a voltage-sensor paddle in KvAP (*22*). In KvAP, there are two distinct segments of S3, termed S3a and S3b. In Kv1.2, the electron density for S3 appears to be a single helix with a bend, presumably near the connection between S3a and S3b. This finding probably represents a different positioning of the paddle from that which we observed in KvAP. Here we do not distinguish between S3a and S3b in Kv1.2, but simply refer to the antiparallel unit formed by the S3 and S4 helices as the voltage-sensor paddle.

The comparison of Kv1.2 and KvAP serves many useful purposes. First, their fundamental similarity reinforces our confidence in the accuracy of the Kv1.2 voltage-sensor model and shows that S4 and S3 form a voltage-sensor paddle as in KvAP. Second, because Kv1.2 and KvAP are similar, we can consider KvAP functional data in constraining possible motions of the Kv1.2 voltage sensor. Third, certain differences between their structures may provide useful information about movements of the voltage sensor. For example, the voltage-sensor paddles in Kv1.2 are in a slightly different position with respect to the S1 and S2 helices (Fig. 2B). This is understandable if the paddles are mobile, allowing them to move in the gating process. Fourth, S4 (and S3) is nearly two helical turns longer at its extracellular end in Kv1.2 than in KvAP (the Kv1.2 S4 contains two extra helical turns preceding the Arg residues) (compare Fig. 2, A and C). This means the paddle in Kv1.2 will project further into the extracellular solution and therefore may exhibit differences (relative to KvAP) in accessibility to spider toxins and small molecules that interact with the voltage sensor from outside the cell.

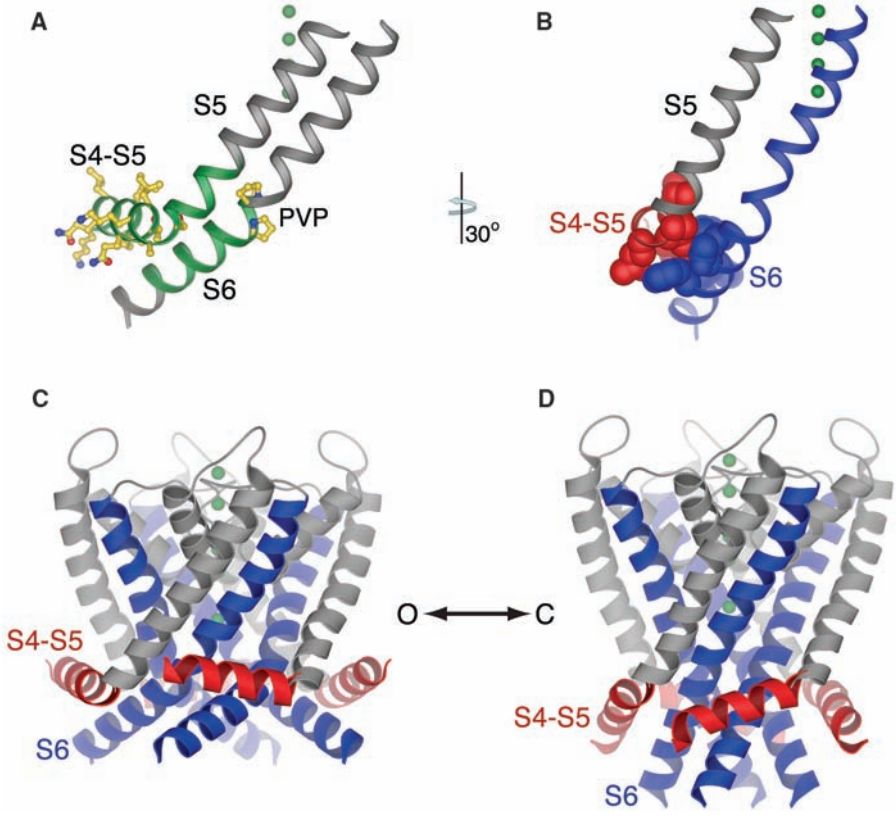

Fig. 3. The connection between the voltage sensor and the pore in the Kv1.2 channel. (**A**) The S6 inner helix (residues 388 to 421) is shown as a gray and green ribbon with yellow side chains for Pro-Val-Pro (residues 405 to 407), and the S4-S5 linker and S5 from the same subunit (residues 311 to 342) are shown as a gray and green ribbon. Side chains on the S4-S5 linker are yellow (carbon), red (oxygen), and blue (nitrogen). The perspective is from the side of the channel near the intracellular water (below)/membrane (above) interface. Regions colored green were necessary to transfer the *Shaker* voltage sensor to KcsA (*32*). (**B**) Residues on the S4-S5 linker in direct contact with residues on S6 are shown as red and blue spheres, respectively. The helices are drawn as ribbons and colored in the following manner: S4-S5, red; S5, gray; and S6, blue. (**C**) A view of the channel tetramer showing the S4-S5 (red), S5 (gray), and S6 (blue) helices as ribbons. The perspective is from the side of the channel with the extracellular side above and the intracellular side below. (**D**) Hypothetical model of the Kv1.2 channel with a closed activation gate, showing the S4-S5, S5, and S6 helices colored as in (C). To generate this model, the inner (S6) helices were adjusted from their observed open conformation in (C) to match the inner helices of the KcsA structure (PDB ID 1K4C), which has a closed activation gate. The S4-S5 linkers were then positioned to maintain the interaction with S6 shown in (A) and (B). The transition from an open to closed activation gate results in a downward displacement (toward the intracellular solution) of the amino-terminal end of the S4-S5 linker. A queue of K^+ ions (green spheres) from the pore are shown as a reference in (A) to (D). The figure was generated with Molscript (*42*).

Voltage-sensor coupling to the pore: The S4-S5 linker helix. The S4-S5 linker is an amphipathic α helix that runs parallel to the membrane plane inside the cell, with its hydrophobic surface facing the membrane and its polar surface facing the cytoplasm (Figs. 2A and 3A). The most important aspect of this helix is its position against the pore; it crosses over the top of the S6 inner helix from the same subunit and makes many amino acid contacts with it (Fig. 3, A and B). The S6 inner helix, by curving parallel to the membrane plane, makes a platform or "receptor" for the S4-S5 helix. This allows us to understand why the S6 helix of Kv channels has the sequence Pro-X-Pro, where X is any amino acid (*Shaker* Kv channels), or Gly in the corresponding region (many other Kv channels): to allow the inner helices to curve so they can form the

correct interaction with the S4-S5 linker helix. This interaction is essential for the coupling of voltage-sensor movements to pore opening and closing, which is depicted in Fig. 3, C and D.

Mutations in the Pro-X-Pro sequence and in the S4-S5 linker helix of *Shaker* Kv channels (*27*–*31*) have profound effects on gating, which have been described as uncoupling the pore from the voltage sensor. One mutational study leaves little doubt about the correctness and importance of the interaction we see between the S4-S5 linker and the S6 inner helix observed in the Kv1.2 crystal structure. Lu *et al*. characterized the amino acid sequence requirements for engineering voltage dependence into KcsA, an otherwise voltage-independent K^+ channel (*21*, *32*). They found they had to transfer to KcsA the *Shaker* Kv channel voltage sensor (S1 to S4), the S4-S5 linker, and the C-terminal end of S6. The required segment of S6 corresponds precisely to the region that makes contact with the S4-S5 linker helix in the Kv1.2 structure (Fig. 3A, in green). Their experiments showed that this interface, formed by the S4-S5 helix against the S6 inner helix, is both necessary and sufficient to reconstruct a functioning voltage sensor on the pore.

Lipid environment of the voltage sensor. The specific interaction between the S4-S5 linker helix and S6 has important consequences for the location of the voltage sensor relative to the pore. Because the linker runs across to the neighboring subunit, the voltage-sensor domains are located at the corners of the square-shaped pore, and they are adjacent to the pore-forming helices of a neighboring subunit (Figs. 2A and 4A). The resulting position of S4 (adjacent to S5 from a neighboring subunit) is in good agreement with the disulfide cross-bridge studies of Papazian and colleagues (*33*). Several studies have attempted to determine the distances separating the first Arg residue on the S4 helix from adjacent and diagonal subunits (*18*, *19*). Here we measure these distances (between C_α carbons) to be 45 and 64 Å, respectively. The position of the voltage sensors at the corners of the pore is reminiscent of a model proposed by Sivaprasadarao and colleagues, but in their model, the voltage sensor contacts the pore of its own subunit rather than the pore of the neighboring subunit (*34*).

The most important consequence of being at the corners of the pore is that the voltage sensors appear to be floating as separate domains from the pore. Aside from the S4-S5 linker interaction with S6, the contacts between a voltage sensor and the pore are not substantial; the tilted S1 helix touches S5 in one place near the extracellular membrane surface, and the S4 helix, which is supposed to move with channel gating, leans against the outer edge of S5 but is not packed tightly against it (Fig. 4, A to C). In a membrane, much of the space separating the hydrophobic surfaces of the pore and the voltage sensor would undoubtedly be filled with lipid molecules (Fig. 4, B and C).

The relative independence of the voltage-sensor domains with respect to the pore in the crystal structure is consistent with several key observations on voltage-sensor function. An independent domain relationship explains why it is possible to transfer a voltage sensor to a non–voltage-dependent K^+ channel (providing that the complementary surfaces at the linker are satisfied) (*21*), why the voltage sensors of KvAP can be expressed in isolation (*22*), and why nature has been able to exploit the S1 to S4 voltage-sensor domain (in the absence of an ion channel pore) to control the activity of a phosphatase enzyme in the cytoplasm (*35*). The existence of a voltage-dependent phosphatase enzyme is a direct demonstration by nature that a protein wall formed by the pore on one side of S4 is not necessary for the voltage sensor to function. All by itself, this simple arrangement of S1 to S4 helices must be able to undergo a voltage-dependent conformational change in the membrane.

Where are the gating-charge Arg residues on the voltage sensor? Studies of the *Shaker* Kv channel have shown that the first four Arg residues (termed Arg 1 through 4 counting from the extracellular side of S4: residues 294, 297, 300, and 303 in Kv1.2) account for most of the gating charge (*5*, *6*), and these residues are the most conserved among voltage sensors from different Kv channels. The chemical environment of these amino acids on the voltage sensor is a mechanistically important and much-debated issue. In the crystal structure, Arg 1 and 2 are located on the voltage sensor's lipid-facing surface (Fig. 4D and Fig. 5, A and B). The first may be near enough to the mem-

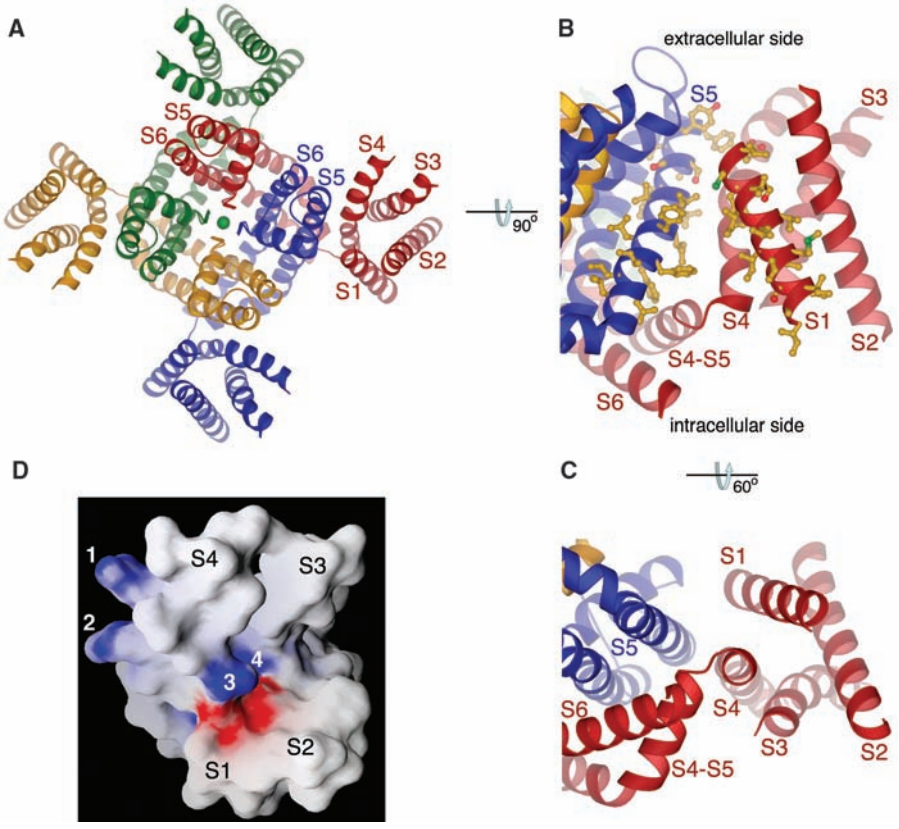

Fig. 4. Views of the integral membrane components (pore and voltage sensors) of the Kv1.2 channel. (**A**) Overall structure of the tetramer, viewed from the extracellular solution, shown as ribbons. Each of the four subunits is colored uniquely. The transmembrane helices S1 to S6 are labeled for the subunit colored in red. Each S4 helix (red, for example) is nearest the S5 helix of a neighboring subunit (blue, for example). (**B**) A close-up view of a voltage sensor and its relationship to the pore, viewed from the side. Side chains for residues on the S1 helix and the S5 helix from the neighboring subunit are shown as sticks and colored according to atom type: carbon, yellow; nitrogen, blue; oxygen, red; and sulfur, green. (**C**) View of the voltage sensor and pore from (B), rotated 60° around the horizontal axis to look down the S4 helix from the intracellular solution. This orientation highlights the minimal contacts between the voltage sensor and pore. (**D**) Surface representation of the S1-to-S4 voltage-sensor domain without the pore, viewed from the extracellular solution in the same orientation as the voltage sensor colored red in (A). The surface is colored red (negative) and blue (positive) for qualitative assessment of the electrostatic potential at the surface. The Arg residues on S4 are numbered 1 to 4. Electrostatic potential was calculated with GRASP software (*43*). In parts (B) and (D), the residues on S1, S2, and S4 were given complete side chains, even though some of them are modeled as polyalanine in the final coordinates. Parts (A) to (C) were generated with Molscript (*42*).

brane surface to extend to the phospholipid head-group layer, whereas the second is somewhat deeper. Arg residues 3 and 4 face helices S1 and S2, where they can make salt bridge interactions with acidic amino acids (Fig. 4D). These four Arg positions in the structure are in agreement with electron paramagnetic resonance (EPR) data on the KvAP channel in lipid membranes (*36*). Although the authors of the EPR study concluded that the Arg residues are buried, their data actually show a lipid environment for the first Arg, a lipid and water mixed environment for the second Arg, and a protein (neither lipid nor water) environment for Arg residues 3 and 4 (*36*, *37*). The correlation between the crystal structure and EPR data argues that the first two of the four highly conserved S4 Arg residues are exposed to lipid in the open conformation of the voltage sensor (see below).

Mechanism of voltage-dependent gating. Two aspects of the Kv1.2 crystal structure suggest that we have determined an open conformation of the channel. First, the inner helix bundle (activation gate) of the pore is opened to ~12 Å in diameter (Fig. 3C). Second, the voltage sensors appear to be in an open position (Fig. 5, A and B); that is, when opening, the voltage sensors move the gating-charge Arg residues nearer to the extracellular side of the cell membrane. This is where we find the Arg residues in the structure if we imagine the channel embedded in a membrane—all four are above the midpoint of the membrane (Fig. 5, A and B).

How might the channel close? Mere inspection of the structure evokes a mechanism (Fig. 5A). In a closed conformation, the inner helix bundle of the pore is expected to be closed as in KcsA, and the voltage sensors are expected to be in a position that will bring the gating-charge Arg residues closer to the intracellular side of the membrane. An inward displacement of the S4 helices (downward in Fig. 5A) will bring the Arg residues toward the intracellular side of the membrane, and at the same time, it will push down on the S4-S5 linker helices. The S4-S5 linker helices will then compress the inner helices and close the pore (Fig. 3D). At a qualitative level, one can understand how a transmembrane electric field, by working on the positive Arg charges on S4, can open the pore when the membrane is positive inside (pushing the charges out) and close the pore when the membrane is negative inside (drawing the charges in).

Many important details have not been specified in the simplified description above, but the process is constrained by further data. One constraint on S4 movements in membranes comes from studies of avidin accessibility to biotin that is tethered on the KvAP channel. These studies have shown that the voltage-sensor paddle in KvAP (helices S3b and S4) is uniquely mobile and that a segment of the S4 helix moves a distance of more than 15 Å through the thickness of the membrane (*23*, *24*). We know, for example, that positions on S4 (marked by black and blue spheres in Fig. 5B) come within a few angstroms of the extracellular and intracellular solutions, respectively, when the voltage sensors move (*24*). The black sphere is near the extracellular side in the open crystal structure of Kv1.2. In a closed conformation, the blue sphere would have to move to the level of the S4-S5 linker, a displacement of at least 15 Å from its position in the crystal structure. The measured accessibility of cysteine residues on S4 of the *Shaker* channel to water-soluble sulfhydryl reagents is consistent with the biotin-avidin data on KvAP (*14*–*16*). S4 movements of this magnitude would transfer the Arg residues far enough to account for the large gating charge associated with *Shaker* Kv channel opening (*4*) and to account for the conformational changes required to open and close the pore (Fig. 3, C and D).

Another constraint comes from the observation that an antiparallel relationship between S3b and S4 has so far been observed in every crystal structure of KvAP (*22*) (see also PDB ID 2A0L), and now we observe a similar relationship between S3 and S4 in Kv1.2. We therefore suppose that S3 and S4 move together as a voltage-sensor paddle unit. We imagine that to close the channel, the paddle undergoes a motion with respect to S1 and S2, with S3 remaining "above" (on the extracellular side of S4) and S4 "below," closer to the intracellular solution. The comparison of the voltage-sensor structure of Kv1.2 and the isolated voltage-sensor structure of KvAP (Fig. 2B, gray and blue traces) offers a suggestion of how a voltage-sensor paddle might begin to move away from its open conformation as a channel begins to close.

It has been argued that accessibility to the top (C-terminal half) of S3 from the extracellular solution in the closed conformation is inconsistent with motions of a voltage-sensor paddle (*38*). But these arguments are based on the perception that the top of S3 in the paddle moves near to the intracellular side and be-

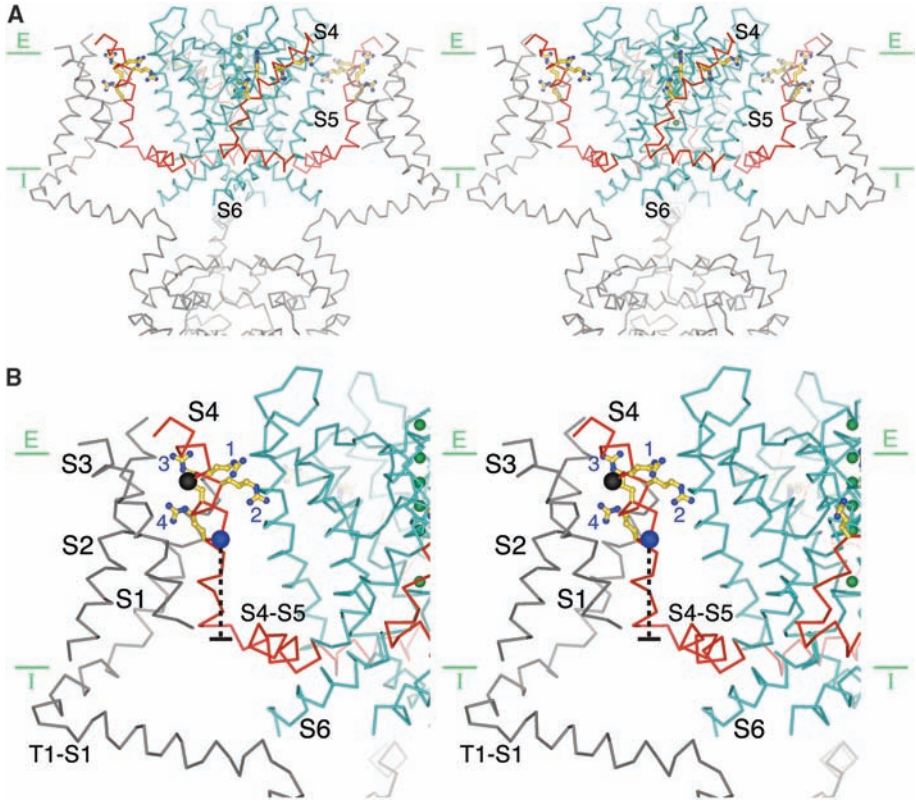

Fig. 5. Stereoview of the Kv1.2 channel showing the pore, voltage sensors, and half of the T1 domain. (**A**) The protein main chain is represented as a C_α trace. The pore is shown in cyan; the S4 helix and the S4-S5 linker in red; and voltage-sensor helices S1 to S3, the T1-S1 linker, and the T1 domain (bottom) in gray. Side chains of Arg 1 to 4 on the S4 helix are shown. α helices S1 to S3, the T1-S1 linker, and the T1 domain are removed from the subunit nearest the viewer. Green lines labeled E (extracellular) and I (intracellular) mark the approximate boundaries of a membrane 30 Å thick. (**B**) An enlarged stereoview of one voltage sensor is shown with the same orientation and coloring as in (A). A black sphere at position 295 highlights that the α carbon of the equivalent amino acid in KvAP approaches within a few angstroms of the extracellular solution (top) when the channel is opened at depolarized membrane voltages (positive inside), as assessed through avidin capture of tethered biotin (*24*). A blue sphere at position 302 shows that the equivalent position in KvAP approaches within a few angstroms of the intracellular solution (approximate distance shown as dashed line) when the channel is closed at negative membrane voltages (negative inside). The figure was generated with Molscript (*42*).

comes completely buried by the hydrophobic core of the lipid membrane (*39*, *40*). In fact, the biotin-avidin studies on KvAP indicate that the top of S3 (S3b in KvAP) does not penetrate deeper than the membrane's outer leaflet (*23*, *24*). Thus, we do not expect there to be a complete hydrophobic core covering this region in the closed conformation. The top of S3 should remain chemically and electrically near the extracellular side.

We hypothesize that S3 of the voltage-sensor paddle serves two important functions: to provide rigidity to S4 and to oppose the inward (closure) movement of the voltage sensor. The C-terminal end of S3 in the voltage-sensor paddle should be more stable at the membrane interface (than in the hydrophobic core) because it contains a mixture of hydrophobic and hydrophilic amino acids. Therefore, at negative membrane voltages, the inward movement of the paddle must always oppose the energetic preference of S3 for the interface. In this way, S3 in the voltage-sensor paddle might serve as a recoil device, causing the voltage sensor to spring to its open conformation when the membrane is depolarized.

Discussion. Crystals of the Kv1.2 K^+ channel provide a view of a Kv channel with its voltage sensors in an apparently native conformation. The electron density for the voltage sensors is weak, but along with information from structures of KvAP, many important questions are answered by the Kv1.2 structure. In particular, three important ideas about voltage-dependent gating are conveyed.

First, a Kv channel is not composed of a rigid disk of α helices in the membrane. Rather, the voltage sensors are self-contained domains, quite independent of the pore except for their specific localized attachments (through the S4-S5 linker) that enable them to perform mechanical work on the pore. In this respect, the voltage-sensor domains are structurally analogous to the ligand-binding domains of ligand-gated ion channels, which are attached to the pore but are separate from it. Instead of being outside the membrane, as in the case of ligand-binding domains, the voltage-sensor domains are membrane-spanning. The Kv channel is the only membrane protein that we know of so far to contain separate domains within the membrane, but others will no doubt be identified in the future. A self-contained voltage sensor means that S4 is not buried in a protein-lined canaliculus. All charge shielding from the membrane and compensation by counter-charges must come from within the voltage-sensor domain itself. We see that the Arg-containing S4 helix is shielded on one face by the S1 and S2 helices of the voltage sensor and is exposed to lipid on the opposite face (Fig. 4 and Fig. 5). A self-contained voltage sensor also means that the position of the voltage sensor with respect to the pore could vary somewhat among different Kv channels. In KvAP, in which the position of the voltage sensors is not constrained by a connection of S1 to a T1 domain, EPR studies show that S1 is mostly buried in protein, rather than exposed to lipid (*36*). This observation can be explained if, in KvAP, the voltage-sensor domains are repositioned slightly (i.e., rotated) to bury S1 between the voltage-sensor domain and the pore (Fig. 4A). Such a repositioning is possible without disrupting the S4-S5 linker's attachment to S6, and although the voltage-sensor paddle would be brought further out on the perimeter, the degree to which S4 is shielded would be unchanged, because the shielding is provided by S1 and S2 of the domain itself.

Second, the Kv1.2 structure shows us how conformational changes within the voltage sensors are transmitted to the pore (Fig. 3, C and D, and Fig. 5, A and B). This is an aspect of voltage-dependent gating that, until now, has eluded a mechanical explanation. The mechanism, depicted in Figs. 3 and 5, is simple: Motions of the S4 helices are transmitted to the inner helix bundle (activation gate) via the S4-S5 linker helices. This is perhaps one of the most straightforward, understandable mechanical systems observed in a protein. When inspecting the Kv1.2 structure, it is at first surprising to see that the voltage sensors are essentially "domain swapped" to the opposite side of neighboring subunits (Fig. 4A). But this arrangement actually permits the S4-S5 linker to form its mechanical attachment to the S6 inner helix, allowing the voltage sensors to perform mechanical work on the pore.

Third, in the open conformation, Arg residues 1 and 2 are on the lipid-exposed surface of the voltage sensor, and Arg residues 3 and 4 are in a position to interact with acidic amino acids inside the domain, between the voltage-sensor paddle (S3 and S4) and voltage-sensor helices S1 and S2. We think that an energetic balance between electrostatic and hydrophobic forces is important for the function of voltage sensors (*25*).

The Kv1.2 structure offers an explanation for many experimental results and ideas that, until now, have seemed contradictory. The original working model based on the KvAP crystal structures is substantially refined by the Kv1.2 structure, but of course this is still a working model, to be modified as new data are obtained. The question of how the voltage sensor moves from the open conformation that we now see to a closed conformation will require further study. This new structure should help in designing the next-stage experiments to test voltage-sensor movements.

References and Notes

1. F. J. Sigworth, *Q. Rev. Biophys.* **27**, 1 (1994).
2. C. M. Armstrong, F. Bezanilla, *J. Gen. Physiol.* **63**, 533 (1974).
3. F. Bezanilla, *Physiol. Rev.* **80**, 555 (2000).
4. N. E. Schoppa, K. McCormack, M. A. Tanouye, F. J. Sigworth, *Science* **255**, 1712 (1992).
5. S. K. Aggarwal, R. MacKinnon, *Neuron* **16**, 1169 (1996).
6. S. A. Seoh, D. Sigg, D. M. Papazian, F. Bezanilla, *Neuron* **16**, 1159 (1996).
7. F. Bezanilla, *J. Gen. Physiol.* **120**, 465 (2002).
8. R. Horn, *J. Gen. Physiol.* **120**, 449 (2002).
9. C. S. Gandhi, E. Y. Isacoff, *J. Gen. Physiol.* **120**, 455 (2002).
10. M. Laine, D. M. Papazian, B. Roux, *FEBS Lett.* **564**, 257 (2004).
11. F. Elinder, P. Arhem, H. P. Larsson, *Biophys. J.* **80**, 1802 (2001).
12. Y. Li-Smerin, D. H. Hackos, K. J. Swartz, *Neuron* **25**, 411 (2000).
13. N. Yang, A. L. George Jr., R. Horn, *Neuron* **16**, 113 (1996).
14. L. M. Mannuzzu, M. M. Moronne, E. Y. Isacoff, *Science* **271**, 213 (1996).
15. S. P. Yusaf, D. Wray, A. Sivaprasadarao, *Pflugers Arch.* **433**, 91 (1996).
16. O. S. Baker, H. P. Larsson, L. M. Mannuzzu, E. Y. Isacoff, *Neuron* **20**, 1283 (1998).
17. H. P. Larsson, O. S. Baker, D. S. Dhillon, E. Y. Isacoff, *Neuron* **16**, 387 (1996).
18. A. Cha, G. E. Snyder, P. R. Selvin, F. Bezanilla, *Nature* **402**, 809 (1999).
19. K. S. Glauner, L. M. Mannuzzu, C. S. Gandhi, E. Y. Isacoff, *Nature* **402**, 813 (1999).
20. D. M. Starace, F. Bezanilla, *Nature* **427**, 548 (2004).
21. Z. Lu, A. M. Klem, Y. Ramu, *Nature* **413**, 809 (2001).
22. Y. Jiang *et al.*, *Nature* **423**, 33 (2003).
23. Y. Jiang, V. Ruta, J. Chen, A. Lee, R. MacKinnon, *Nature* **423**, 42 (2003).
24. V. Ruta, thesis, Rockefeller University (2005).
25. T. Hessa, S. H. White, G. von Heijne, *Science* **307**, 1427 (2005).
26. S. B. Long, E. B. Campbell, R. MacKinnon, *Science* **309**, 897 (2005); published online 7 July 2005 (10.1126/science.1116269).
27. Y. Liu, M. Holmgren, M. E. Jurman, G. Yellen, *Neuron* **19**, 175 (1997).
28. N. E. Schoppa, F. J. Sigworth, *J. Gen. Physiol.* **111**, 295 (1998).
29. D. H. Hackos, T. H. Chang, K. J. Swartz, *J. Gen. Physiol.* **119**, 521 (2002).
30. O. Yifrach, R. MacKinnon, *Cell* **111**, 231 (2002).
31. M. Sukhareva, D. H. Hackos, K. J. Swartz, *J. Gen. Physiol.* **122**, 541 (2003).
32. Z. Lu, A. M. Klem, Y. Ramu, *J. Gen. Physiol.* **120**, 663 (2002).
33. M. Laine *et al.*, *Neuron* **39**, 467 (2003).
34. D. J. Elliott *et al.*, *EMBO J.* **23**, 4717 (2004).
35. Y. Murata, H. Iwasaki, M. Sasaki, K. Inaba, Y. Okamura, *Nature* **435**, 1239 (2005).
36. L. G. Cuello, D. M. Cortes, E. Perozo, *Science* **306**, 491 (2004).
37. R. MacKinnon, *Science* **306**, 1304 (2004).
38. C. S. Gandhi, E. Clark, E. Loots, A. Pralle, E. Y. Isacoff, *Neuron* **40**, 515 (2003).
39. H. C. Lee, J. M. Wang, K. J. Swartz, *Neuron* **40**, 527 (2003).
40. C. Gonzalez, F. J. Morera, E. Rosenmann, O. Alvarez, R. Latorre, *Proc. Natl. Acad. Sci. U.S.A.* **102**, 5020 (2005).
41. A. T. Brunger *et al.*, *Acta Crystallogr.* **D54**, 905 (1998).
42. P. Kraulis, *J. Appl. Crystallogr.* **24**, 946 (1991).
43. A. Nicholls, K. A. Sharp, B. Honig, *Proteins* **11**, 281 (1991).

44. We thank A. Lee, V. Ruta, and members of the MacKinnon laboratory for helpful discussions; R. Jain for initial experiments with lipids; R. Dutzler for assistance with data collection; O. Pongs for Kv1.2 DNA; J. Trimmer for β2 subunit DNA; Brookhaven National Laboratory (National Synchrotron Light Source beamlines X25 and X29) and the Swiss Light Source (beamline PX1) staff for assistance in data collection; and W. Chin for help with manuscript preparation. This work was supported in part by NIH grant no. GM43949 to R.M. R.M. is an Investigator in the Howard Hughes Medical Institute. Atomic coordinates and structure factors have been deposited in the Protein Data Bank with accession ID 2A79.

17 June 2005; accepted 5 July 2005
Published online 7 July 2005;
10.1126/science.1116270
Include this information when citing this paper.